RESEARCH ARTICLE

Enhanced capacity of LiCoO$_2$ and graphite battery by using methylene methanedisulfonate as electrolyte additive

Jue Wu[1] · Hongyan Qiu[1] · Jianhao Zhang[1] · Zhipeng Zhuang[1] · Xianhe Wang[1]

Abstract

Lithium cobalt oxide (LiCoO$_2$) and graphite-based Li-ion batteries have been widely applied for consumer electronics because of the long cycle life and easy preparation. However, the limited capacity for traditional materials hampers the practical application for high energy-density battery. Conventional electrolyte system could not satisfy the need for high-capacity materials. Here, methylene methanedisulfonate (MMDS) was chosen as electrolyte additive for enhancing the available capacity for LiCoO$_2$ and graphite-based battery. The effect of MMDS on the LiCoO$_2$ cathode and graphite anode was investigated via multi electrochemical methods. It was found that the capacity for cells with MMDS electrolyte additive increases (from 142.6 mAh g^{-1} for pristine to 193.4 mAh g^{-1} on LiCoO$_2$/Li battery, from 275.5 mAh g^{-1} for pristine to 407.0 mAh g^{-1} on graphite/Li battery). The experimental results indicate that improved capacity by MMDS electrolyte additive can be attributable to the stabilized interface on both cathode and anode sides, leading to superior interfacial Li$^+$ kinetics and mitigated bulk structural degradation, which was further confirmed by the *ex-situ* electrochemical and structural characterization.

Graphical abstract

Keywords Layered cathode · lithium-ion batteries · Capacity · Kinetics

1 Introduction

Benefits from high energy density and excellent cyclability, lithium-ion batteries (LIBs) have been widely applied in portable mobile devices and electric vehicles [1, 2]. For lithium-ion batteries, the energy density mainly depends on the practical capacity and working voltage of active materials [3]. Lithium cobalt oxide (LiCoO$_2$, LCO) cathode and graphite (C) anode have been used for lithium-ion batteries in commercial based on the suitable capacity and excellent cyclability [4, 5]. Generally, LCO presents an available capacity of around 130 mAh g^{-1} when charged to 4.2 V (vs. Li/Li$^+$), which could be further enhanced with increased cut-off voltage (4.5 V vs. Li/Li$^+$) [6, 7]. However, the utilization

✉ Jue Wu
  jwu@zcst.edu.cn

1 School of Applied Chemistry and Materials, Zhuhai College of Science and Technology, Zhuhai 519041, China

of LCO cathode at high voltage remains a tough challenge since it would lead to side reactions at the electrode/electrolyte interface and severe structural degradation [6, 8]. The currently available electrolyte based on the $LiPF_6$ salt is unstable and decomposes to HF, and induces transition metal dissolution, leading to cell failure. Therefore, the alternative electrolytes with much-improved stability and capacity are urgently needed.

Considering the cost and procedures, modifying electrolyte has been applied as a promising approach to control the electrode/electrolyte interface film, such as electrolyte additive [6, 7, 9, 10], dual-salt and dual-solvent electrolytes [11, 12]. The electrolyte should be stable enough at the high voltage, the surface electrode should be protected by some kind of protective layers that prevent undesirable side reactions [11]. In the dual-salt electrolyte system, the synergistic effect between the salts and/or the solvents helps to form a protective layer on the electrode [11, 13]. Some well-known electrolyte additives (such as fluoroethylene carbonate (FEC)), which can prolong the lifetime of cells, have been studied by many researchers [14]. Among various electrolyte additives, methylene methanedisulfonate (MMDS) has been studied as a functional additive to improve the electrochemical performance of cells [15–20], providing enhanced capacity, high Coulombic efficiency, low impedance, and long cycling life in electrochemical performance. Ex situ characterization results confirmed that MMDS has a positive effect on forming a stabilized solid electrolyte interphase (SEI) film, which could mitigate capacity fading and enhance cycle life [18, 21].

Although it has been studied by many researchers, the role of MMDS on the cathode and anode materials has not been clearly investigated. Here, we conducted a study on the effect of MMDS electrolyte additive for both LCO cathode and graphite anode electrodes. Figure 1 shows the structure of MMDS molecular used in this work. MMDS is composed of two SO_3 units with carbon atoms attached to each sulfur atom to form a six-atom symmetric ring structure [19]. According to previous work [16], MMDS modified electrolyte has a lower oxidation potential than conventional

carbonate-based electrolyte, and participates in the formation process of interface film. With this modification, the capacity, cycling performance, and impedance behaviors for LCO/Li and graphite/Li batteries are improved. The X-ray diffraction (XRD), and electrochemical impedance spectroscopy (EIS) characterization results reveal that these improvements benefit from the stabilized bulk and interfacial structure. The effect of MMDS on electronic/ionic transport properties was investigated via electrochemical impedance spectroscopy (EIS) and cyclic voltammograms (CV), the modified battery delivers enhanced kinetics on the charge transfer reaction at the electrode/electrolyte interface.

2 Experimental section

2.1 Preparation of electrolyte

The base electrolyte consists of 1 M $LiPF_6$ in ethylene carbonate (EC), diethyl carbonate (DEC), and ethyl methyl carbonate (EMC) (1:1:1 by vol%). The MMDS was purchased from Shanghai Macklin Biochemical Technology Co., Ltd. The MMDS modified electrolyte was prepared via adding a certain mass fraction (0.0, 0.2, 0.5, and 1.0%) of MMDS to the base electrolyte, and named as 0.0% MMDS, 0.2% MMDS, 0.5% MMDS, and 1.0% MMDS.

2.2 Electrochemical measurements

The LCO/Li CR2025 coin type half cells were assembled with LCO as cathode active material, celgard 2325 as separator, and Li metal as counter electrode, along with 100 μL electrolyte. The loading mass for the cathode active material is 3.0–5.0 mg. The cells were assembled in Ar-gas filled glove box. The graphite/Li CR2025 coin type half cells were assembled with graphite as anode active material, Li metal as counter electrode, and the others were the same as $LiCoO_2$/Li half cells.

The assembled half cells were tested via a Neware CT-4008T test chamber (Shenzhen, China) at room temperature. For the LCO/Li half cells, the cells were cycled at 0.1, 0.2, and 0.5 C (1 C = 200 mA g^{-1}) for three cycles, respectively, then cycled at 1 C for the following cycling in the voltage range of 3.2–4.3 V. The cyclic voltammetry (CV) tests were conducted at the voltage region of 3.2–4.3 V at scan rate of 0.1 mV s^{-1}. For the graphite/Li half cells, the cells were cycled at 0.2 C, 0.4 C, and 1.0 C (1 C = 100 mA g^{-1}) for three cycles, respectively, and then cycled at 2 C for the following cycling in the voltage range of 0.005-1.5 V. The CV tests were conducted at the voltage region of 0.005–1.5 V at different scan rates (0.3, 0.4, 0.5, 0.6, and 0.7 mV s^{-1}). The electrochemical impedance spectroscopy (EIS)
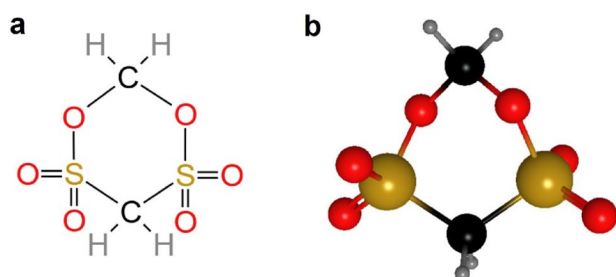

Fig. 1 **a** The molecule structure and **b** configuration for the electrolyte additive methylene methanedisulfonate (MMDS)

measurements were conducted under a voltage amplitude of ± 5 mV and frequency range between 10^{-2} and 10^{5} Hz.

2.3 Physical characterizations

The morphology of electrode materials was probed via scanning electron microscopy (SEM, Tescan). X-ray diffraction (XRD, Rigaku Ultima IV) technique was used to probe the structural evolution during the cycling process, using a Cu K_α radiation ($\lambda = 1.5406$ Å) source with a scan rate of 15°/min between 10° and 90°.

3 Results and discussion

3.1 Characterization of LiCoO$_2$ and graphite materials

The morphology of the pristine LCO and graphite material was probed by scanning electron microscopy (SEM). As shown in Fig. 2a, the cathode active material of LCO consists of micron-sized particles with well-defined surfaces. Besides, the anode active material of graphite presents a clean surface with sharp edges (Fig. 2b). The bulk structure for the pristine LCO and C materials was probed via the XRD technique. Figure 2c presents the XRD patterns for pristine LCO powder. The diffraction peaks can be ascribed to the typical layered structure of α-NaFeO$_2$ (PDF#77-1370) with a space group of $R\bar{3}m$ [22]. The diffraction
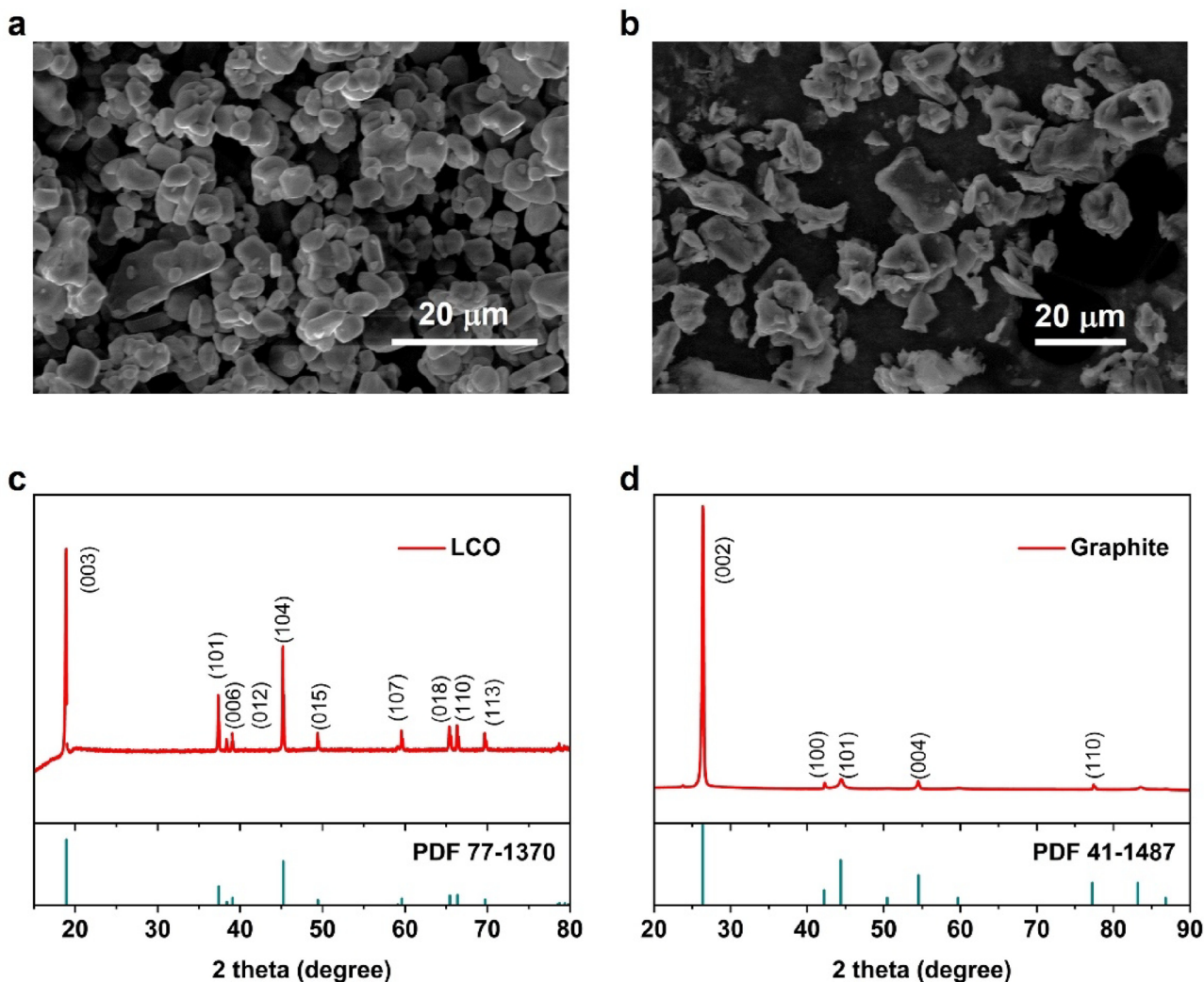

Fig. 2 The SEM images for **a** the pristine LCO oxide powder and **b** graphite powder. XRD patterns for **c** the pristine LCO oxide and **d** graphite powder

peaks are sharp without residual peaks, which indicates the formed structure is well-crystallized without impure phase. Figure 2d shows the XRD patterns of pristine graphite material, the major diffraction peaks can be indexed to the intercalated graphite structure (PDF#41-1487).

3.2 Electrochemical performance of LiCoO₂ cathode

Figure 3 presents the initial charge–discharge curves of LiCoO₂/Li cell without and with variable concentrations of MMDS with the voltage window of 3.2–4.3 V. All curves deliver a characterization of LCO material without large change, which means the MMDS additive does not affect the lithium (de) intercalation process [6]. As shown in Fig. 3a, under a current density of 20 mA g⁻¹, the available capacity of the LiCoO₂/Li cell with base electrolyte is 142.6 mAh g⁻¹ with Coulombic efficiency of 73.9%. It suggests a large amount of irreversible lithium consumption during the charging process [23]. After MMDS additive modification, the available capacity was enhanced. The initial discharge capacity with 0.2, 0.5, and 1.0% MMDS is 175.8, 194.3, and 179.4 mAh g⁻¹, respectively. It suggests that the CEI (Cathode electrolyte interface) film was optimized with MMDS electrolyte additive modification. However, the available capacity decreases upon the content of MMDS increased to 1.0%. This indicates that an excessive amount of MMDS additive would lead to a thicker CEI film [16, 21], which hinders the Li ions diffusion [23].
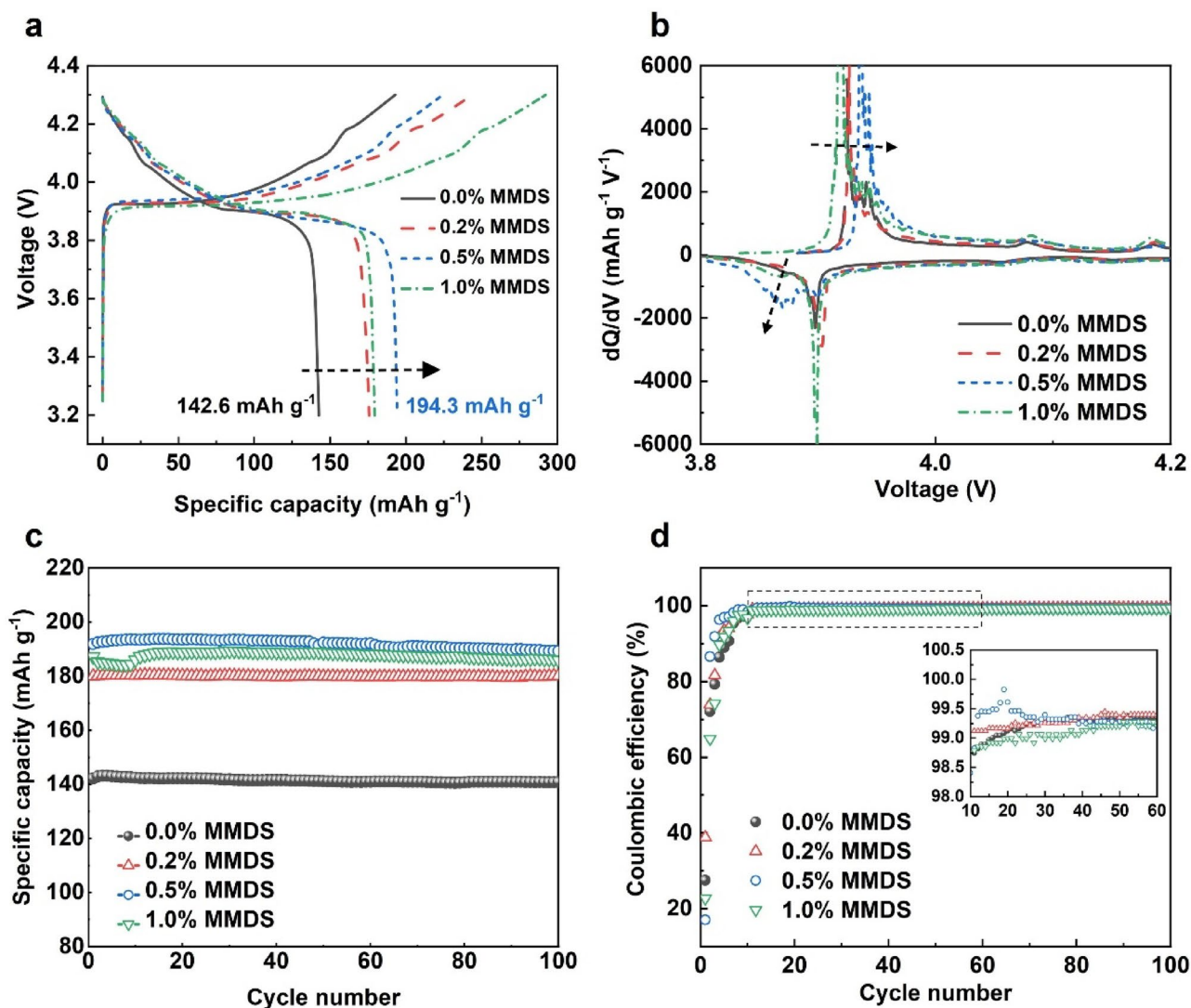

Fig. 3 Electrochemical performance for LiCoO₂/Li half cell. **a** Charge–discharge curves under the voltage window of 3.2–4.3 V and current density of 20 mA g⁻¹, and **b** corresponding differential capacity versus voltage (dQ/dV) curves. **c** Specific capacity under the voltage window of 3.2–4.3 V and current density of 100 mA g⁻¹ and **d** Coulombic efficiency during the initial 100 cycling

Figure 3b delivers the differential capacity versus voltage (dQ/dV) curves of LiCoO₂/Li cells. The dQ/dV curves show the main peaks at potentials of 3.9 V vs. Li/Li⁺. For the MMDS modified cells, the oxidation peak (3.9 V vs. Li/Li⁺) shifts to a higher voltage, and the reduction peak at (3.9 V vs. Li/Li⁺) shifts to a lower voltage. It indicates that the increased polarization, which might be due to the CEI film formed on the electrode surface, hinders reversible lithium ions (de) intercalation [24]. Figure 3c and d shows the cycling performance of the LiCoO₂/Li cells using the electrolyte without/with MMDS additive. During 100 cycles charge–discharge process, the LCO with electrolyte additive has a higher capacity than those of cells with base electrolyte (185.9 mAh g⁻¹ for 0.5% MMDS additive vs. 140.8 mAh g⁻¹ for base electrolyte at the 100th cycle). Figure S1 shows

cells with 0.5% MMDS additive deliver higher capacity at different rates than that of cells with base electrolyte.

3.3 Electrochemical performance of graphite anode

The role of MMDS additive on the electrochemical performance for graphite anode was also studied. Figure 4a delivers the charge–discharge curves for graphite/Li cell with voltage window between 0.001 and 1.5 V. All curves deliver a characterization of graphite material without large change, which means the MMDS additive does not affect the lithium (de)intercalation process. During the charge process, the plateau at 0.75 V suggests irreversible electrolyte decomposition. Pristine graphite/Li cell delivers an available capacity of 275.5 mAh g⁻¹. After 0.5% MMDS
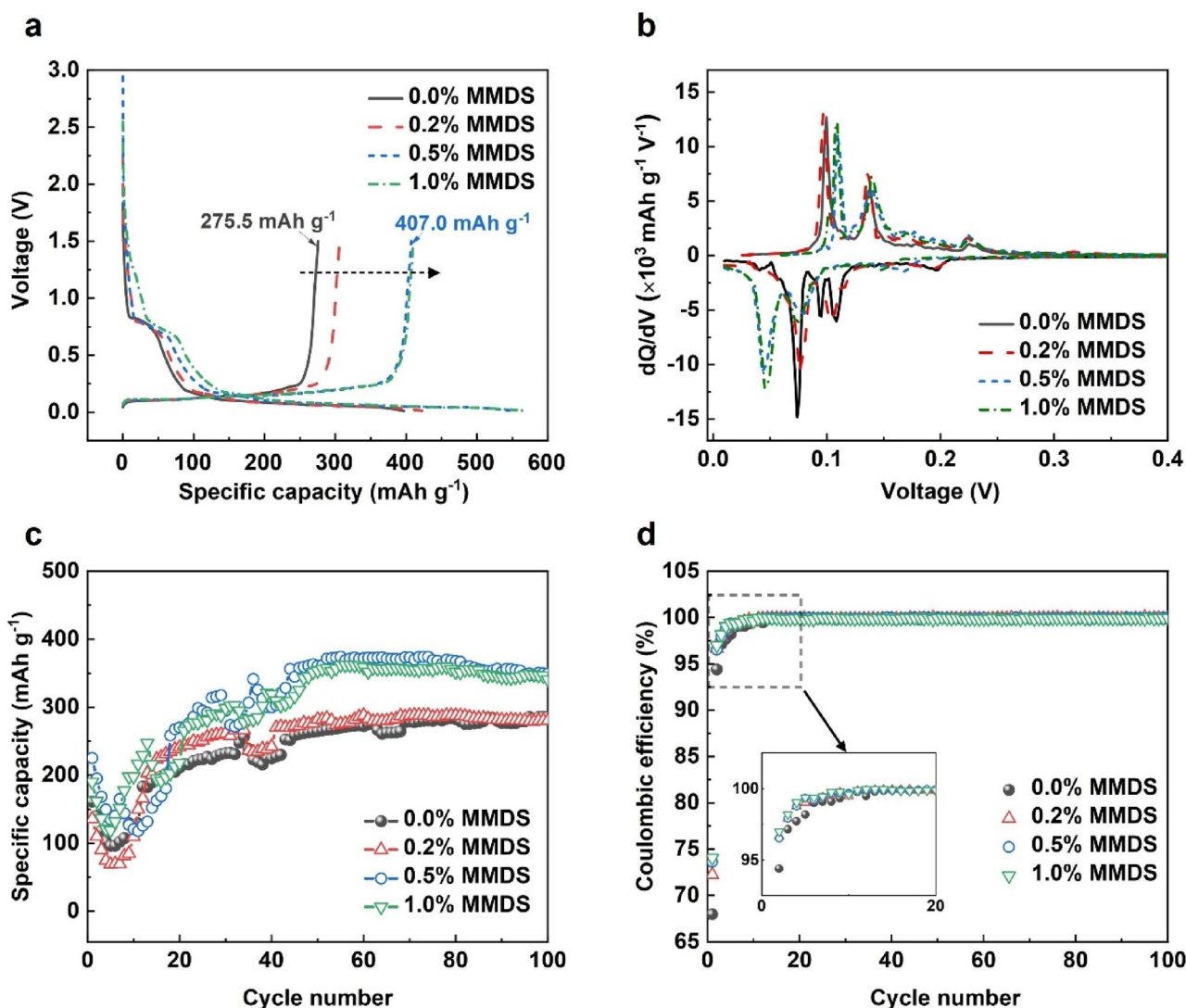

Fig. 4 Electrochemical performance for graphite/Li battery. **a** The charge–discharge curves with the voltage window of 0.001–1.5 V and current density of 20 mA g⁻¹ and **b** corresponding differential capacity versus voltage (dQ/dV) curves. **c** Specific capacity with the voltage window of 0.001–1.5 V and current density of 100 mA g⁻¹ and **d** Coulombic efficiency during the 100 cycling

electrolyte additive was added, the discharge capacity increased to 407.0 mAh g^{-1}. Figure 4b shows the dQ/dV curves based on Fig. 4a data. For the oxidation peaks, cell with MMDS shifts to a higher voltage. For comparison, the reduction peaks shift to a lower voltage with MMDS additive. During the cycling process, the MMDS additive modified cell exhibits higher reversible capacities than those cells with base electrolyte, indicating its improved cycling performance (Fig. 4c). It is worth noting that the capacity decrease in around the initial ten cycles might be related to the side reaction [25], which needs further study. After 100 cycles, the available capacity for 0.0, 0.2, 0.5, and 1.0% MMDS is 285.7, 280.4, 349.6, and 340.7 mAh g^{-1}, respectively. Figure 4d shows the Coulombic efficiency during cycling for graphite/Li cells using base and MMDS additive modified electrolyte. The MMDS modified cells

deliver higher Coulombic efficiency than that of cells with base electrolyte. The Coulombic efficiency of cells with 0.0, 0.2, 0.5, and 1.0% MMDS is 68, 72, 74, and 74%, respectively. These results suggest that the MMDS additive could facilitate the formation of SEI, which improves the cycling stability by preventing the graphite exploration.

3.4 Interfacial and bulk structure evolution during cycling

Electrochemical impedance spectroscopy (EIS) was applied here to probe the electrochemical processes on the electrode/electrolyte interface. Figure 5a and b; Table 1 present Nyquist plots and the corresponding resistance evolution of the LCO/Li cells at pristine and after long cycles at room temperature. The Nyquist plots are consisted of semicircles
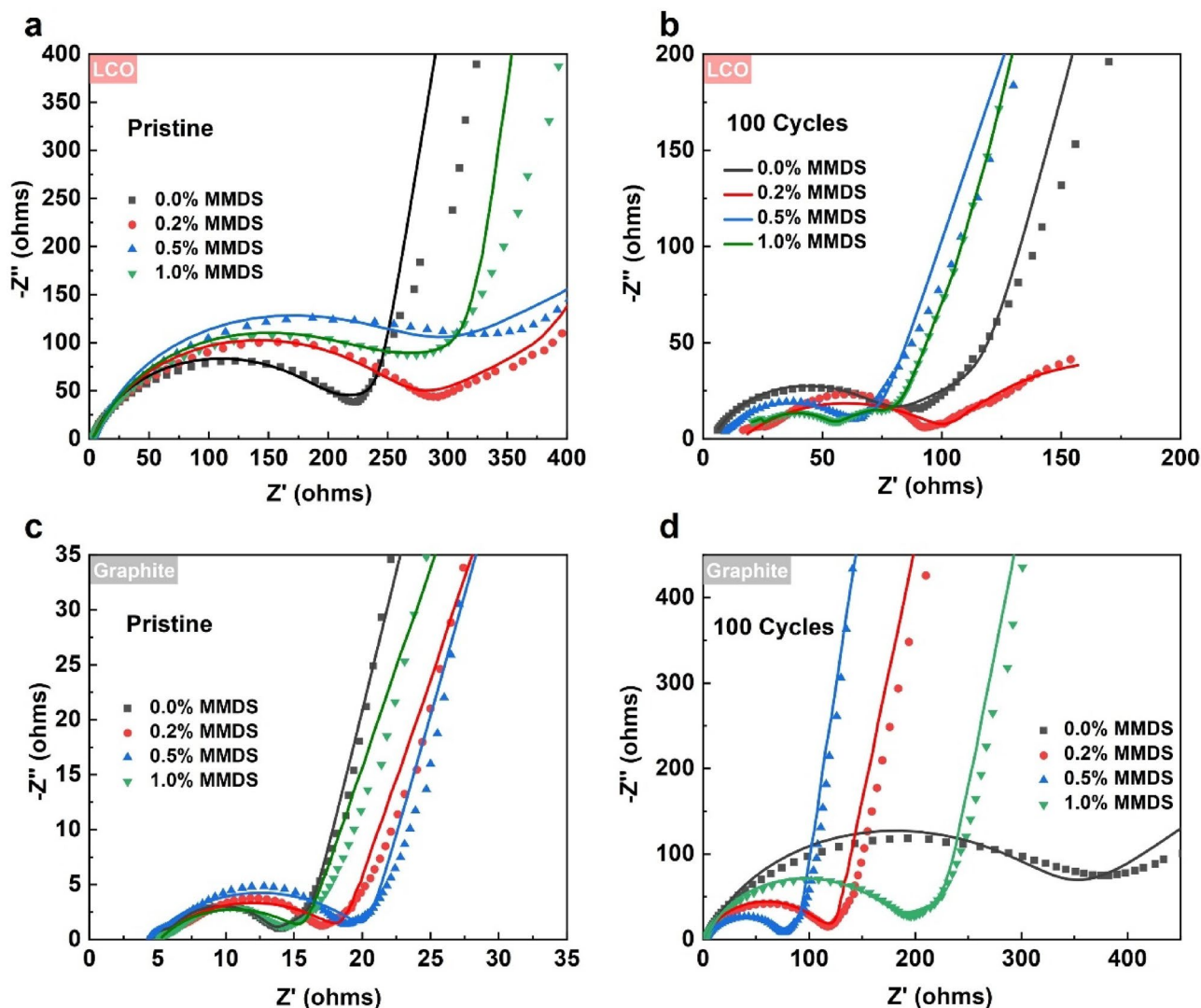

Fig. 5 Interfacial evolution probed via ex situ EIS test. The EIS data **a** before cycling, and **b** after cycling for LCO/Li battery with/without MMDS additives. The EIS data **c** before cycling, and **d** after cycling for graphite/Li battery with/without MMDS electrolyte additives

Table 1 The fitted R_f and R_{ct} values from EIS data for LCO/Li battery

Sample	Pristine R_{ct}/Ω	100 cycles R_f/Ω	100 cycles R_{ct}/Ω
0.0% MMDS	183.9	8.451	81.40
0.2% MMDS	367.5	6.296	42.49
0.5% MMDS	236.0	7.696	47.07
1.0% MMDS	205.1	3.683	67.09

Table 2 The fitted R_f and R_{ct} values from EIS data for graphite/Li battery

Sample	Pristine R_{ct}/Ω	100 cycles R_f/Ω	100 cycles R_{ct}/Ω
0.0% MMDS	7.108	2.587	336.4
0.2% MMDS	8.567	2.488	138.9
0.5% MMDS	11.200	2.479	81.33
1.0% MMDS	9.236	2.327	168.8

and a slop line. According to the previous work [26], the semicircle at high-frequency region can be attributed to lithium ions diffusion through the electrode/electrolyte interface film, and the semicircle at middle-frequency region can be ascribed to the charge transfer process at the cathode/electrolyte interface, and the inclined line at low-frequency region can be assigned to the lithium ions diffusion in the electrode [17]. The equivalent circuit was applied to fit the Nyquist spectra in Figure S2 [27]. Before cycling, the semicircles for MMDS modified cell are larger than those with base electrolyte, which indicates the cells with MMDS modification deliver higher resistance, which suggests additive decomposition (Fig. 5a). After cycling, the R_{ct} resistance for cells with 0.0 (base), 0.2, 0.5, and 1.0% MMDS is 81.40, 42.49, 47.07, and 67.09 Ω, respectively (Fig. 5b). Obviously, the R_{ct} resistance for MMDS modified cells is smaller than those for cells with base electrolyte. It indicates the undesired electrode/electrolyte interface reaction in the LiCoO$_2$/Li cells can be mitigated with MMDS as an electrolyte additive, leading to a more stable interface [16, 21].

Electrochemical impedance spectroscopy (EIS) was also applied to probe the interfacial reaction at anode side. Figure 5c and d; Table 2 deliver Nyquist plots and the resistance evolution of the graphite/Li cells at pristine and after 100 cycles at room temperature. Before cycling, the semicircles for MMDS modified cells are larger than those for cells with base electrolyte, which indicates the cells with MMDS modification deliver higher resistance, which suggests additive decomposition (Fig. 5c). After cycling, the R_{ct} resistance for cells with 0.0 (base), 0.2, 0.5, and 1.0% MMDS is 336.4, 138.9, 81.33, and 168.8 Ω, respectively (Fig. 5d). Obviously, the R_{ct} resistance for cells with additive is smaller than that of cells without additives. Combined with previous reports [28], the MMDS additive modified

cell is suggested to deliver stabilized electrode/electrolyte interface.

Figure 6a displays the cyclic voltammograms (CV) of LCO/Li cells in electrolytes without and with 0.2, 0.5, and 1.0% MMDS additives. The cell without MMDS additive delivers an oxidation peak at around 4.01 V and a reduction peak at 3.86 V. Concerning the electrolyte with MMDS added, the oxidation peaks deliver increased peak current with higher voltage potential (4.054 V, 4.036 V, and 4.109 V for 0.2, 0.5 and 1.0% MMDS, respectively). Meanwhile, the cathodic peaks deliver increased peak current with lower voltage potential. The CV profiles clearly show the effect of MMDS additive, which effectively accelerates the higher amount of lithium ions intercalation. The increased polarization suggests that an excellent CEI film formed with MMDS added electrolyte, which is consistent with the increased R_{ct} in Fig. 5. The cyclic voltammograms of graphite/Li cells are presented in Fig. 6b. The cell with base electrolyte delivers an oxidation peak at around 0.34 V, and a reduction peak at around 0.15 V. The current increased with the MMDS electrolyte additive added, which indicates the accelerated lithium ions intercalation process, consistent with the charge–discharge curves.

Figure 6c, d and e, and f displays the cyclic voltammograms (CV) of cycled LCO/Li cell in electrolyte without and with 1.0% MMDS additives under different scanning rates. As shown in Fig. 6c and e, the peak intensity of anodic/cathodic peak increases with the enhanced scanning rate. Based on the CV profiles with different scanning rates, I_p–$\nu^{1/2}$ profiles deliver the fitting slope which correlated with the Li ions diffusion [29, 30]. For cells without additives, the slope for the anodic peak and the cathodic peak is 0.0021 and 0.0013, respectively (Fig. 6d and f). For comparison, the cell with 0.5% MMDS additives ensures higher slope for the anodic peak and cathodic peak (0.036 and 0.0027). The CV profiles clearly show the positive effect of MMDS additive on the kinetics of lithium ions diffusion.

Besides, Fig. 7 displays the cyclic voltammograms (CV) of graphite/Li cell in electrolyte without and with 1.0% MMDS additives under different scanning rates. In Fig. 7a and b, the peak intensity of anodic/cathodic peak increases with the enhanced scanning rate. Based on the CV profiles with different scanning rates, I_p–$\nu^{1/2}$ profiles deliver the fitting slope which correlated with the Li ions diffusion [29, 30]. For cells without additives, the slope for the anodic peak and the cathodic peak is 0.1348 and 0.0939, respectively (Fig. 7c and d). For comparison, the cell with 1.0% MMDS additives ensures higher slope for anodic peak and cathodic peak (0.1551 and 0.1196). The CV profiles clearly show the positive effect of MMDS additive on the kinetics of lithium ions diffusion.
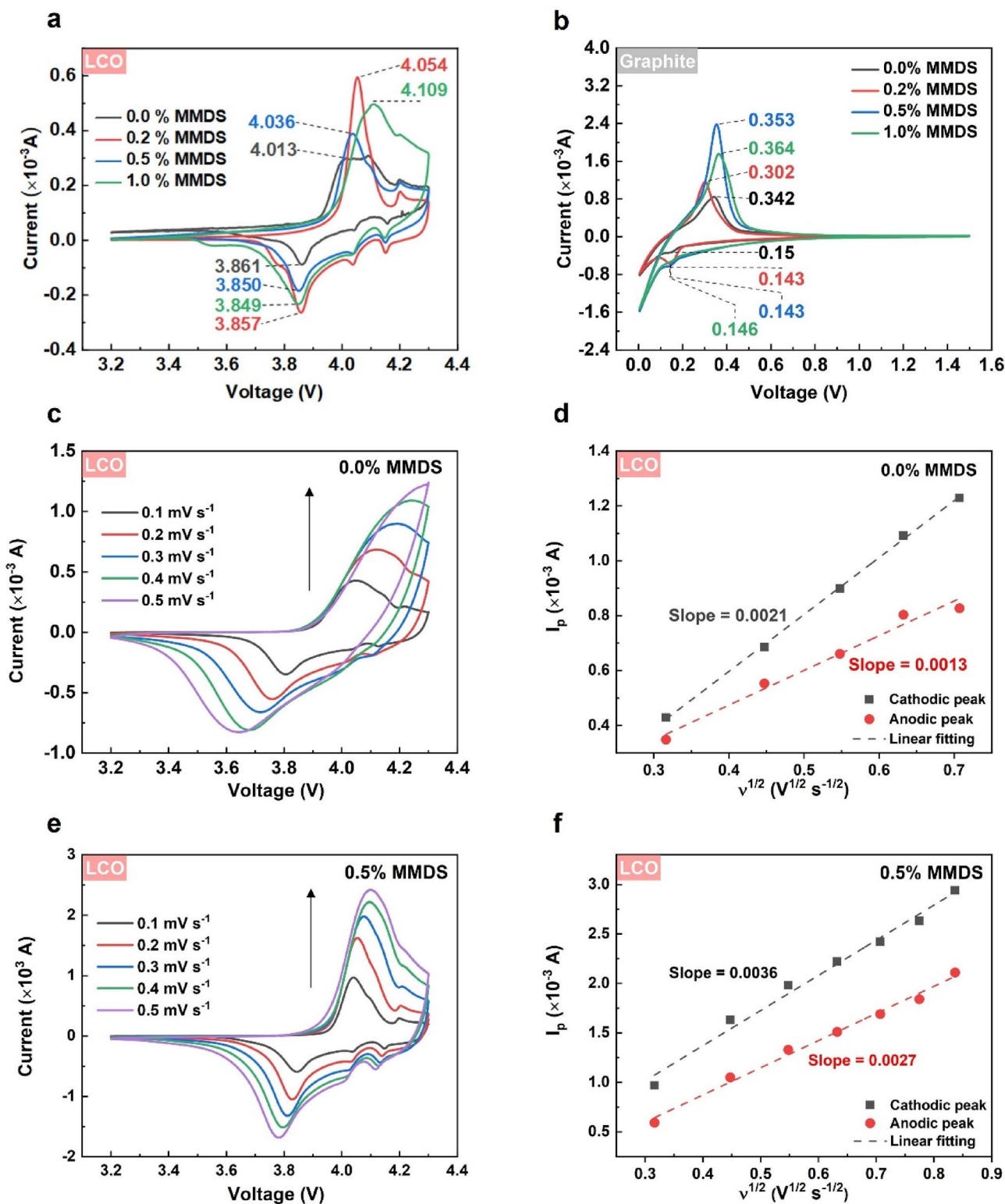
Fig. 6 Cyclic voltammograms of **a** LCO/Li cell, and **b** graphite/Li cell with 0.0, 0.2, 0.5, and 1.0% MMDS modification, respectively. Cyclic voltammograms and fitting results of LCO/Li cell after 100 cycles **c**, **d** without MMDS, **e**, **f** with 0.5% MMDS at various scan rates (0.1, 0.2, 0.3, 0.4, and 0.5 mV s^{-1})
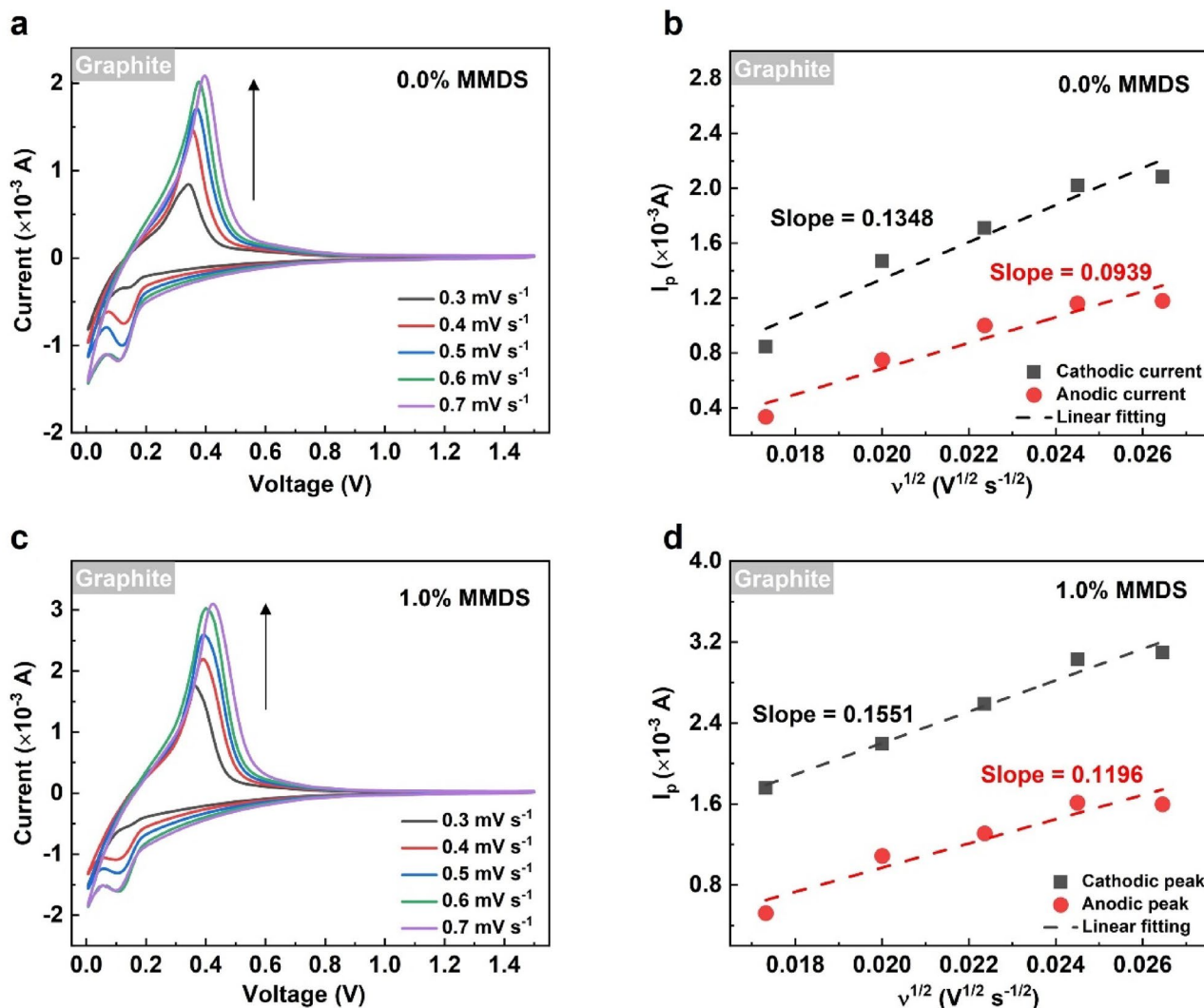
Fig. 7 Cyclic voltammograms and fitting results of graphite/Li cell **a**, **b** without MMDS, **c**, **d** with 1.0% MMDS at various scan rates (0.3, 0.4, 0.5, 0.6, and 0.7 mV s^{-1})

The effect of MMDS on the bulk structural stability of the LCO electrode and graphite electrode is further probed by the ex situ X-ray diffraction (XRD) technique (Fig. 8a, S3). Compared to that in the base electrolyte, the diffraction peak shift of (003) diffraction peak for LCO cathode (0.12° for 0.5% MMDS, and 0.32° for 0.0% MMDS) decreases with MMDS additive modification, revealing the positive effect of electrolyte additive on structural stability for LCO cathode material [31]. Figure 8b shows ex situ XRD patterns of graphite anode with/without electrolyte additive. For pristine graphite material, it delivers a (002) diffraction peak at $2\theta = 26.5°$, which could be ascribed to an interlayer distance of 3.36 Å for graphite [32]. After the discharge process, the (002) diffraction peak shifts to lower diffraction angles because of lattice expansion [32]. Therefore, the *ex-situ* XRD result on the graphite anode also reveals the

sustained structural evolution due to less peak shift of (002) diffraction peak (0.12° for 0.5% MMDS, and 0.34° for 0.0% MMDS) with MMDS additive modification (Fig. 8b, S4).

4 Conclusions

In summary, the role of MMDS electrolyte additive on the LiCoO$_2$ cathode and graphite anode has been investigated. The electrochemical performance of LiCoO$_2$ and graphite electrodes could be improved with MMDS as an electrolyte additive. According to the experimental results, the enhanced capacity can be ascribed to the optimized SEI/CEI film for both the anode and cathode sides, which could mitigate the electrolyte decomposition, deliver superior interfacial Li$^+$ kinetics, and protect the bulk structural degradation.
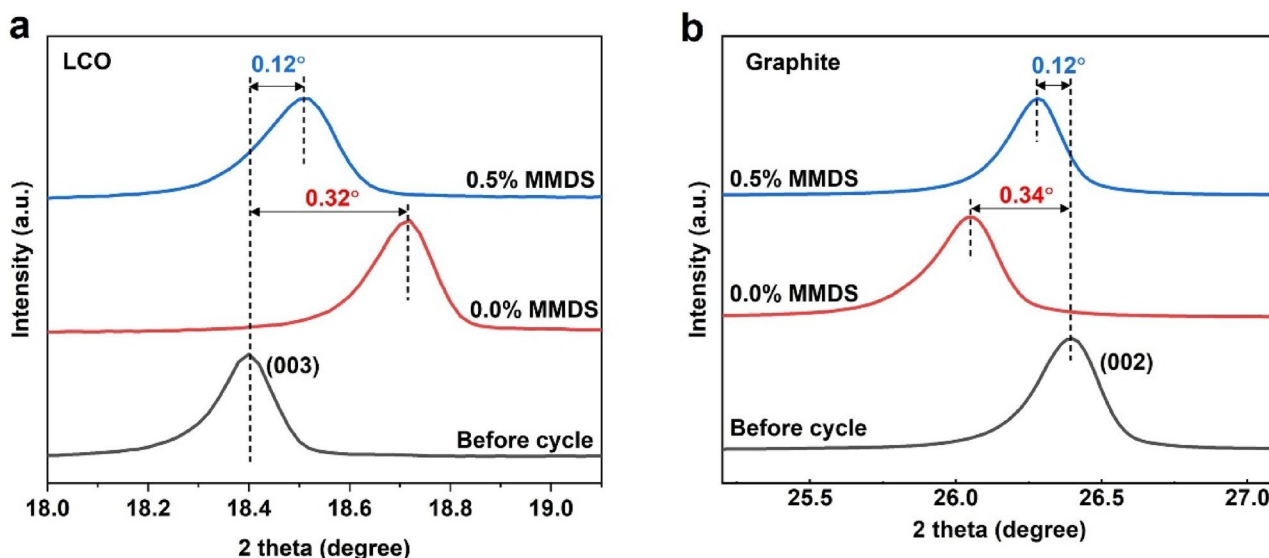
Fig. 8 Bulk evolution probed via ex situ XRD. XRD patterns of **a** LCO cathode, and **b** graphite anode at pristine and after 100 cycles with/without MMDS electrolyte additive

Therefore, the MMDS modified LCO exhibits a high capacity of 193.4 mAh g^{-1}, and modified graphite delivers a higher capacity of 407.0 mAh g^{-1}. This work provides a simple way to improve the electrochemical performance for lithium ions battery materials.

Author contributions JW and HQ designed, carried out the experiments, and performed the data analyses. Beyond that, JW wrote the manuscript. JZ helped to perform the analysis with constructive discussions. ZZ and XW help to polish and revise the manuscript. All the authors reviewed the manuscript.

Data availability No datasets were generated or analyzed during the current study.

Declarations

Conflict of interest The authors declare no conflicts of interest.

References

1. Kim T, Song W, Son D-Y, Ono LK, Qi Y (2019) Lithium-ion batteries: outlook on present, future, and hybridized technologies. J Mater Chem A 7(7):2942–2964
2. Lee W, Muhammad S, Sergey C, Lee H, Yoon J, Kang YM, Yoon WS (2020) Advances in the cathode materials for lithium rechargeable batteries. Angew Chem-Int Ed 59(7):2578–2605
3. Yi H, Liang Y, Qian Y, Feng Y, Li Z, Zhang X (2023) Low-cost Mn-based cathode materials for lithium-ion batteries. Batteries 9(5):246
4. Etacheri V, Marom R, Elazari R, Salitra G, Aurbach D (2011) Challenges in the development of advanced Li-ion batteries: a review. Energy Environ Sci 4(9):3243–3262
5. Tarascon J-M (2010) Key challenges in future Li-battery research. Philosophical Trans Royal Soc A: Math Phys Eng Sci 368(1923):3227–3241
6. Yang X, Lin M, Zheng G, Wu J, Wang X, Ren F, Zhang W, Liao Y, Zhao W, Zhang Z, Xu N, Yang W, Yang Y (2020) Enabling stable high-voltage LiCoO$_2$ operation by using synergetic interfacial modification strategy. Adv Funct Mater 30(43):2004664
7. Yang X, Wang C, Yan P, Jiao T, Hao J, Jiang Y, Ren F, Zhang W, Zheng J, Cheng Y, Wang X, Yang W, Zhu J, Pan S, Lin M, Zeng L, Gong Z, Li J, Yang Y (2022) Pushing lithium cobalt oxides to 4.7 V by lattice-matched interfacial engineering. Adv Energy Mater 12(23):2200197
8. Cai M, Dong Y, Xie M, Dong W, Dong C, Dai P, Zhang H, Wang X, Sun X, Zhang S, Yoon M, Xu H, Ge Y, Li J, Huang F (2023) Stalling oxygen evolution in high-voltage cathodes by lanthurization. Nat Energy 8(2):159–168
9. Fan X, Wang C (2021) High-voltage liquid electrolytes for Li batteries: progress and perspectives. Chem Soc Rev 50(18):10486–10566
10. Xu K (2014) Electrolytes and interphases in Li-ion batteries and beyond. Chem Rev 114(23):11503–11618
11. Beyene TT, Su W-N, Hwang BJ (2022) Dilute dual-salt electrolyte for successful passivation of in-situ deposited Li anode and permit effective cycling of high voltage anode free batteries. J Power Sources 542:231752
12. Hagos TM, Berhe GB, Hagos TT, Bezabh HK, Abrha LH, Beyene TT, Huang C-J, Yang Y-W, Su W-N, Dai H, Hwang B-J (2019) Dual electrolyte additives of potassium

hexafluorophosphate and tris (trimethylsilyl) phosphite for anode-free lithium metal batteries. Electrochim Acta 316:52–59

13. Beyene TT, Bezabh HK, Weret MA, Hagos TM, Huang C-J, Wang C-H, Su W-N, Dai H, Hwang B-J (2019) Concentrated dual-salt electrolyte to stabilize Li metal and increase cycle life of anode free Li-metal batteries. J Electrochem Soc 166(8):A1501

14. Profatilova IA, Kim S-S, Choi N-S (2009) Enhanced thermal properties of the solid electrolyte interphase formed on graphite in an electrolyte with fluoroethylene carbonate. Electrochim Acta 54(19):4445–4450

15. Bian F, Zhang Z, Yang Y (2014) Enhanced high temperature cycling performance of LiMn2O4/graphite cells with methylene methanedisulfonate (MMDS) as electrolyte additive and its acting mechanism. J Energy Chem 23(3):383–390

16. Zuo X, Fan C, Xiao X, Liu J, Nan J (2012) High-voltage performance of LiCoO$_2$/graphite batteries with methylene methanedisulfonate as electrolyte additive. J Power Sources 219:94–99

17. Cui Y, Yang C, Zhuang Z, Wang M, Zhuang Q (2018) Synthesis and electrochemical performance of spheroid LiNi$_{1/3}$Co$_{1/3}$Mn$_{1/3}$O$_2$ in the electrolyte modified by ethylene sulfate and methylene methanedisulfonate. J Inorg Organomet Polym Mater 28:731–737

18. Wang R, Li X, Zhang B, Wang Z, Guo H (2015) Effect of methylene methanedisulfonate as an additive on the cycling performance of spinel lithium titanate electrode. J Alloys Compd 648:512–520

19. Wang R, Li X, Wang Z, Guo H (2016) Manganese dissolution from LiMn$_2$O$_4$ cathodes at elevated temperature: methylene methanedisulfonate as electrolyte additive. J Solid State Electrochem 20(1):19–28

20. Wang Y, Yu X, Liu Y, Wang Q (2019) Interfacial structure and electrochemical stability of electrolytes: methylene methanedisulfonate as an additive. Phys Chem Chem Phys 21(1):217–223

21. Huang T, Wu M, Wang W, Pan Y, Fang G (2014) Effect of methylene methanedisulfonate as an additive on the cycling performance of LiMn$_2$O$_4$ cathode at elevated temperature. J Power Sources 262:303–309

22. Zhang H, Huang Y, Wang Y, Wang L, Song Z, Wang H, Xu C, Tian X, Wang S, Fang J, Zhao W, Cao H, Yao X, Yang J, Tan R, Yang L, Pan F, Zhao Y (2023) In-situ constructed protective bilayer enabling stable cycling of LiCoO$_2$ cathode at high-voltage. Energy Storage Mater 62:102951

23. Li X, Liu L, Li S, Guo L, Li B, Zhang G (2020) Improving cyclic stability of LiMn$_2$O$_4$/graphite battery under elevated temperature by using 1, 3-propane sultone as electrolyte additive. Front Mater 7:263

24. Sun Y, Tao M, Zou Y, He Z, Su Y, Cheng Y, Zhao D, Zhang X, Zhang Z, Yang Y (2023) 2,2,5,5-Tetramethyl-2,5-disila-1-oxacyclopentane as a bifunctional electrolyte additive for Ni-rich (LiNi$_{0.9}$Co$_{0.05}$Mn$_{0.05}$O$_2$) cathode in Li-ion batteries. J Power Sources 556:232411

25. Wang K, Xing L, Zhi H, Cai Y, Yan Z, Cai D, Zhou H, Li W (2018) High stability graphite/electrolyte interface created by a novel electrolyte additive: a theoretical and experimental study. Electrochim Acta 262:226–232

26. Zhang C, Wan J, Li Y, Zheng S, Zhou K, Wang D, Wang D, Hong C, Gong Z, Yang Y (2020) Restraining the polarization increase of Ni-rich and low-Co cathodes upon cycling by Al-doping. J Mater Chem A 8(14):6893–6901

27. Guo F, Xie Y, Zhang Y (2022) Tuning Li-excess to optimize Ni/Li exchange and improve stability of structure in LiNi$_{0.8}$Co$_{0.1}$Mn$_{0.1}$O$_2$ cathode material for lithium-ion batteries. Nano Res 15(10):8962–8971

28. Mai S, Xu M, Wang Y, Liao X, Lin H, Li W (2014) Methylene methanedisulfonate (MMDS) as a novel SEI forming additive on anode for lithium ion batteries. Int J Electrochem Sci 9(11):6294–6304

29. Deng X, Li M, Ma Z, Wang X (2023) Controllable construction of La$_2$Li$_{0.5}$Co$_{0.5}$O$_4$ multifunctional armor to stabilize Li-rich layered oxide cathode for high-performance lithium-ion batteries. Nano Res 16(7):10634–10643

30. Wu J, Chen Z, Cheng J, Wen Q, Gao W, Wang X, Tuo C (2023) Accelerating Li$^+$ intercalation kinetics through synergetic modification in Li-rich cathode. J Mater Sci 58:16785–16796

31. Wan J, Zhu J, Xiang Y, Zhong G, Liu X, Li Y, Zhang KHL, Hong C, Zheng J, Wang K, Yang Y (2021) Revealing the correlation between structure evolution and electrochemical performance of high-voltage lithium cobalt oxide. J Energy Chem 54:786–794

32. Ma P, Mirmira P, Eng PJ, Son S-B, Bloom ID, Filatov AS, Amanchukwu CV (2022) Co-intercalation-free ether electrolytes for graphitic anodes in lithium-ion batteries. Energy Environ Sci 15(11):4823–4835